Journal of Chromatography B 1268 (2026) 124847

Contents lists available at ScienceDirect

Journal of Chromatography B

journal homepage: www.elsevier.com/locate/jchromb

A reversed-phase HPLC-based dual-parameter assay for the human urinary kallidinogenase enzyme activity

Hong-yan Ge [a], Ya-jun Zhang [b], Jun-qin Qiao [a,*], Li Fan [b], He-liang Fu [b], Hong-zhen Lian [a,*]

[a] State Key Laboratory of Analytical Chemistry for Life Science, School of Chemistry & Chemical Engineering and Centre for Shared Scientific Research Facilities, Nanjing University, 163 Xianlin Avenue, Nanjing 210023, China
[b] Jiangsu Aidea Pharmaceutical Co., Ltd, 69 Xinganquan West Road, Yangzhou 225008, China

ARTICLE INFO

Keywords:
Reversed-phase high-performance liquid chromatography (RP-HPLC)
Human urinary kallidinogenase (KN)
Enzyme activity
Substrate
Dual-parameter quantification

ABSTRACT

In this work, a dual-parameter quantification protocol was successfully developed for determining the enzymatic activity of human urinary kallidinogenase (KN) using reversed-phase high-performance liquid chromatography (RP-HPLC). KN serves as a hydrolytic enzyme to cleave the substrate S-2266 (H-D-Val-Leu-Arg-pNA). Effective separation of the product, substrate, and KN was achieved under optimized chromatographic conditions. By minimizing matrix interference through HPLC separation and using multi-wavelength detection, both selectivity and sensitivity were significantly improved. Moreover, the dual-parameter quantification method, which simultaneously measured the formation of reaction products and the consumption of substrates to reflect KN enzyme activity, markedly improved the reliability of the determination. This method was successfully applied to the activity assay of actual KN samples. The established method has been demonstrated to be effective and reliable with comparable greenness. It provides a powerful tool for the quantitative monitoring of KN activity in biological products and paves the way for its application in complex biological matrices.

1. Introduction

Biopharmaceuticals have advanced rapidly in recent years, revolutionizing the pharmaceutical landscape through significant applications, including antibody therapies, vaccines, gene therapy, and targeted treatments [1]. Compared to conventional small-molecule drugs, biopharmaceuticals offer superior therapeutic potential, particularly due to their targeting precision and specificity, making them preferable for the treatment of complex and refractory diseases [2].

Among biopharmaceuticals, protein-based drugs constitute a major class, playing a crucial role in modern therapeutics. This group, which includes hormones, enzymes, antibodies, and growth factors, is widely used in the treatment of various diseases such as cancer [3], autoimmune disorders [4], and metabolic conditions [5].

In biological systems, enzymes serve as chemical catalysts [6], facilitating biochemical reactions with remarkable selectivity, efficiency, and specificity, and are capable of distinguishing structurally similar substrates [7,8]. These attributes make enzymes promising therapeutic agents for protein-based drugs [9]. Enzyme therapies have shown substantial progress in treating genetic disorders, cancer [10], metabolic deficiencies, rheumatic conditions [11], wound healing, inflammation, and other diseases [12]. To date, over 20 enzyme-based therapeutic products have been developed and approved for the treatment of numerous rare and life-threatening diseases [13,14]. Furthermore, enzyme-based gene therapy, post-translational modification strategies for enzymes, and enzyme–nanomaterial conjugates hold significant promise for future therapeutic development [15,16].

Human urinary kallidinogenase, also known as urinary kallikrein (KN) [17], is a serine glycoprotein hydrolase composed of 238 amino acids and extracted from the urine of healthy adult males [18]. It functions by releasing vasoactive kinins from kininogen. KN improves microcirculation in ischemic brain regions, promotes neovascularization, facilitates collateral circulation, and regulates brain tissue metabolism. It has demonstrated significant efficacy in treating acute cerebral infarction and reducing thrombosis [19]. KN is now recognized as an important enzyme-based drug for the treatment of acute thrombotic cerebral infarction of mild to moderate.

For drugs, inadequate dosage may fail to achieve the desired therapeutic effect, whereas an overdosage can lead to immune rejection. For enzyme-based drugs, enzyme activity serves as a key indicator for evaluating both product quality and dosage appropriateness. To ensure the therapeutic efficacy and safety, quality control of KN is crucial not

* Corresponding authors.
E-mail addresses: qiaojunqin@nju.edu.cn (J.-q. Qiao), hzlian@nju.edu.cn (H.-z. Lian).

https://doi.org/10.1016/j.jchromb.2025.124847
Received 25 June 2025; Received in revised form 26 October 2025; Accepted 5 November 2025
Available online 6 November 2025
1570-0232/© 2025 Elsevier B.V. All rights are reserved, including those for text and data mining, AI training, and similar technologies.

only in the final products but also throughout the entire production process. Therefore, the development of a reliable and effective method for quantifying KN activity is essential.

The method for determining KN activity typically relies on ultraviolet-visible spectrophotometry (UV–Vis) [20]. However, this technique suffers from several limitations, such as significant inaccuracies and inconsistent outcomes caused by interference from substrates or matrix in the solution. Similarly, conventional methods for measuring enzyme activity such as fluorescence spectrophotometry [21], electrochemical detection [22], and titration [23] are also susceptible to matrix interference and often yield significant errors in complex matrices. To overcome these limitations, researchers have developed several novel strategies for enzyme activity profiling. For instance, activity-based chemical probes (ABPs), analyzed via SDS-polyacrylamide gel electrophoresis (SDS-PAGE), microscopy, or mass spectrometry, enable selective measurement of specific enzyme activities in vivo [24]. However, their chemical instability, complex synthesis, and limited compatibility in practical applications restrict broader use. Boric acid-based molecularly imprinted polymers (MIPs) have demonstrated effectiveness in selectively capturing enzymes and minimizing matrix interference [25]. Nevertheless, the incomplete removal of template molecules can lead to false positives in subsequent assays. Recently, quantum dots (QDs) and carbon dots (CDs) have been employed as fluorescent sensors offering high sensitivity and versatile surface functionalization for detecting the activity of enzymes [26]. However, these nanomaterials exhibit limited selectivity and remain susceptible to environmental interference. Nuclear Magnetic Resonance (NMR) techniques and Magnetic Resonance Imaging-Chemical Exchange Saturation Transfer (MRI-CEST) have also been applied to enzyme activity detection [27], but their application is limited by high instrumentation costs, operational complexity, and sensitivity to physiological conditions, which compromise signal reliability. In addition, MALDI-TOF-MS, when combined with click chemistry and fluoro-affinity purification, has enabled the detection of cytochrome P450 activity [28]; however, the occurrence of signal hotspots impairs quantitative accuracy. Overall, although these emerging methods offer promising capabilities, each is accompanied by inherent limitations such as low selectivity that hinder their application in the accurate determination of KN activity.

High-performance liquid chromatography (HPLC) is a powerful technique for separating and analyzing complex systems, known for its excellent separation selectivity and high quantitative accuracy. It has been widely applied in environmental science [29], single-cell research [30], biomedicine [31,32], food safety [33,34], as well as in chemistry and chemical engineering [35,36]. In recent years, along with these applications, significant advances in sample preparation [37] and microsampling techniques [38] have greatly enhanced the trace-level detection capability and analytical efficiency of chromatographic methods, enabling rapid and accurate analysis of actual samples. Among various liquid chromatographic modes, reversed-phase high-performance liquid chromatography (RP-HPLC) provides high column efficiency and strong separation capability, making it the predominant technique in many analytical applications. It has gained increasing attention for the separation and analysis of chiral compounds [39], biomacromolecules [40], metabolites [41], and proteomics [42]. Therefore, RP-HPLC represents a promising method for the reliable determination of KN enzymatic activity.

In this study, an RP-HPLC method employing a dual-parameter quantification strategy with crossing validation was developed to evaluate the activity of KN. The enzymatic activity was assessed by simultaneously measuring product formation and substrate consumption resulting from hydrolysis. The chromatographic method demonstrated high sensitivity, accuracy and reliability for determining KN activity, and showed considerable greenness.

2. Materials and methods

2.1. Chemicals and samples

Acetonitrile (ACN, HPLC grade) was purchased from Thermo Fisher Scientific (Waltham, MA, USA). Trifluoroacetic acid (TFA, HPLC grade) and acetic acid (HAc, HPLC grade) were provided by Aladdin Reagent Co., Ltd. (Shanghai, China). Tris-HCl buffer (0.2 mol•L^{-1}, pH 8.0) was obtained from Sangon Biotech Co., Ltd. (Shanghai, China). S-2266 was purchased from Bidepharm Co., Ltd. (Shanghai, China), and p-Nitroaniline (pNA) was obtained from Macklin Biochemical Co., Ltd. (Shanghai, China). Human urinary kallidinogenase (KN) was provided by Aidea Pharmaceutical Co., Ltd. (Yangzhou, China). Ultrapure water (18.25 MΩ•cm), obtained from a Milli-Q water system (Millipore, Bedford, MA, USA), was used throughout the experiment. All the chemicals were of analytical grade unless otherwise stated and were used without further purification.

2.2. Instruments

HPLC analysis was performed on an Agilent 1260 Infinity II LC system with a diode array detector (DAD) (Agilent Technologies, Santa Clara, CA, USA). An ultrasonic cleaning machine SB-5200DTD (YMNL, Nanjing, China), and a thermostatic water bath HH-4D (Yitong, Changzhou, China), were used for sample preparation.

2.3. Chromatographic conditions

HPLC analysis was performed using a TSKgel C4 column (4.6 × 150 mm i.d., 3 μm) (TOSOH, Tokyo, Japan). The mobile phase consisted of acetonitrile (A) and 0.1 % TFA aqueous solution (B), with the gradient elution as follows: 0–5 min, linear gradient from A:B (20:80, *v*/v) to A:B (30:70, v/v); 5–10 min, linear gradient from A:B (30:70, v/v) to A:B (50:50, v/v); 10–15 min, isocratic elution at A:B (50:50, v/v). The column temperature was maintained at 30 °C, and the flow rate was 1.0 mL•min^{-1}. A 10 μL aliquot of each sample solution was injected in triplicate. Detection wavelengths were set at 380 nm for pNA, 315 nm for S-2266, and 280 nm for KN.

2.4. Preparation of experimental and standard solutions

Substrate solution: S-2266 (4.35 mg) was accurately weighed and transferred into a 5 mL volumetric flask. Ultrapure water was added, and the solution was sonicated at room temperature until fully dissolved. The volume was then adjusted to the mark with ultrapure water to yield a 1.5 mmol•L^{-1}substrate solution.

Reaction buffer: Tris-HCl buffer (0.2 mol•L^{-1}, pH 8.0) was used directly as the reaction buffer for enzymatic hydrolysis.

Enzyme reaction stop solution: A 50 % acetic acid solution was prepared by mixing equal volumes of acetic acid and ultrapure water.

Enzyme solution: KN (5.0 mg) was accurately weighed and transferred into a 50 mL volumetric flask. It was dissolved and diluted to the volume with reaction buffer to obtain a KN stock solution. This stock was then serially diluted with reaction buffer to prepare a series of KN solutions (0.5–100 μg•mL^{-1}).

pNA and S-2266 standard solutions: pNA (5.0 mg) and S-2266 (25.0 mg) were accurately weighed and transferred into 50 mL volumetric flasks, respectively. Ultrapure water was added, and the solutions were sonicated at room temperature until fully dissolved. The solutions were then diluted to the volume with ultrapure water to obtain the stock standard solutions. These were further serially diluted with ultrapure water to prepare pNA standard solutions (0.01–100 μg•mL^{-1}) and S-2266 standard solutions (0.25–500 μg•mL^{-1}).

2.5. In vitro enzyme-catalyzed hydrolysis reaction

Reaction solution: 100 μL of KN solution and 1.0 mL of reaction buffer were transferred into a centrifuge tube and incubated at 37 °C for 10 min. Subsequently, 200 μL of the S-2266 substrate solution, pre-heated at 37 °C for 5 min, was added to the enzyme-buffer mixture. The resulting solution was incubated at 37 °C for a specified duration, and the reaction time was precisely recorded. At predetermined time points, 200 μL of enzyme reaction stop solution was added to terminate the reaction. The resulting mixtures were referred to as reaction solution.

Blank solution: 200 μL of enzyme reaction stop solution was first added to the enzyme-buffer mixture. The resulting solution was incubated at 37 °C for a specified duration. At predetermined time points, 200 μL of the substrate solution was added. The resulting mixtures were referred to as blank solution.

Both the reaction solution and blank solution were filtered through 0.45 μm polyethersulfone (PES) syringe filters (Acrodisc, Ann Arbor, MI, USA) and subsequently analyzed using the HPLC method.

3. Results and discussion

3.1. Optimization of chromatographic conditions

3.1.1. Selection of gradient elution programs

KN is a serine protease. The current methodology for assessing the enzymatic activity of KN involves the use of S-2266 (H-D-Val-Leu-Arg-pNA), a chromogenic tripeptide substrate hydrolyzed by KN at the arginine (R) residue, leading to the release of p-nitroaniline (pNA) as product, as illustrated in Fig. 1. Upon completion of the reaction, the resulting solution predominantly contains the product pNA, the unreacted substrate S-2266, and a trace amount of residual KN enzyme.

Since proteins are highly hydrophobic, a reversed-phase C4 chromatographic column was selected to ensure complete elution of KN and to prevent residual retention. Trifluoroacetic acid (TFA) was added to the mobile phase in order to improve the peak shapes of the analytes, thereby enhancing separation efficiency. Due to the significant differences in hydrophobicity among pNA, S-2266, and KN, gradient elution was employed. Eight different gradient elution programs were performed with acetonitrile (ACN) (A) and 0.1 % TFA aqueous solution (B) as the mobile phases. The mixed standard solution of pNA, S-2266, and KN was used to evaluate the applicability of these chromatographic conditions, and the separation results are shown in Fig. S1.

Figs. S1A–E suggested that, as the initial acetonitrile ratio increased, the analytes eluted more rapidly. Although the retention times of analytes under elution conditions D and E were shorter, their resolution values (Table S1) were relatively low, especially for elution condition E. Considering both elution time and resolution, an initial acetonitrile ratio of 20 % was chosen.

We further investigated the separation efficiency by keeping the initial ratio of acetonitrile at 20 % and adjusting the gradient change rate, corresponding to elution conditions C and F—H. Among these, elution condition H provided superior resolution and relatively short retention times, making it more suitable for separation analysis of pNA, S-2266, and KN, even in more complex systems requiring rapid elution. Therefore, elution condition H was selected as the optimal elution condition. The elution program was as follows: 0–5 min, linear gradient from A:B (20:80, *v*/v) to A:B (30:70, v/v); 5–10 min, linear gradient from A:B (30:70, v/v) to A:B (50:50, v/v); 10–15 min, isocratic elution at A:B (50:50, v/v).

Under the optimal condition, standard solutions of the product (pNA), substrate (S-2266) and enzyme (KN) were injected respectively (Fig. 2). The results showed that the retention times of pNA, S-2266, and KN were 4.5 min, 7.7 min, and 11.5 min, respectively, with well-defined peak shapes, displaying excellent separation selectivity.

3.1.2. Selection of detection wavelength

The online DAD spectra revealed that the characteristic absorption

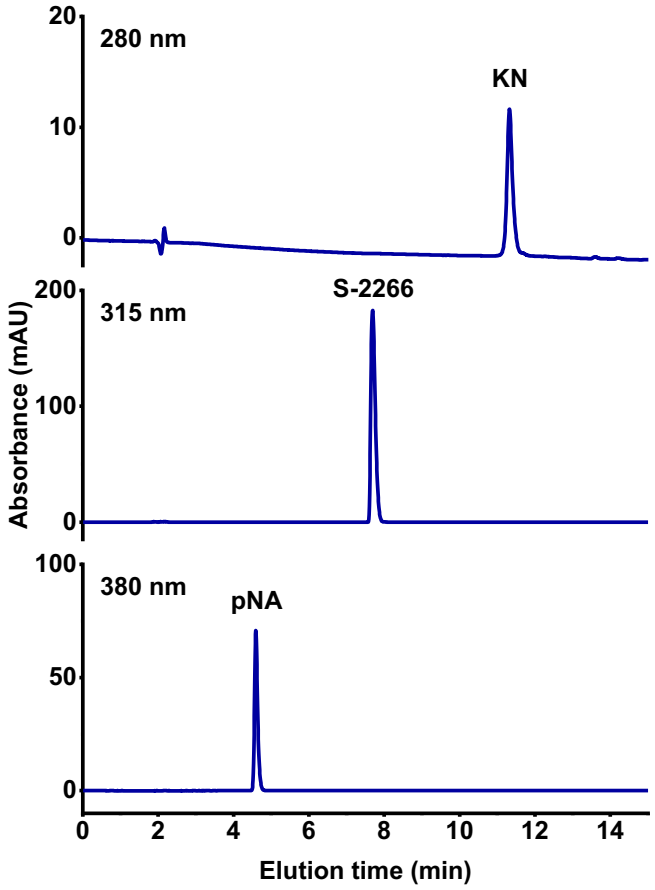

Fig. 2. HPLC chromatograms of the standard solutions of pNA, S-2266, and KN under the optimal condition. Chromatograms were obtained on a TSKgel C4 column (4.6 × 150 mm i.d., 3 μm) at 30 °C, under a gradient condition: 0–5 min, linear gradient from A:B (20:80, *v*/v) to A:B (30:70, v/v); 5–10 min, linear gradient from A:B (30:70, v/v) to A:B (50:50, v/v); 10–15 min, isocratic elution at A:B (50:50, v/v). Mobile phase A was acetonitrile and mobile phase B was 0.1 % TFA aqueous solution at a flow rate of 1.0 mL min^{-1}. 10 μL aliquot of each standard solution was injected. Detection wavelengths were set at 380, 315, and 280 nm for pNA, S-2266, and KN, respectively.

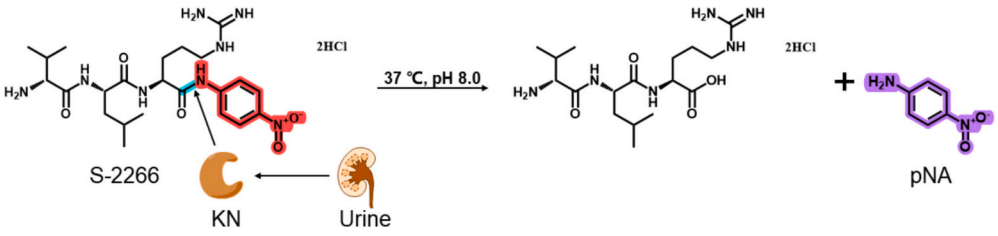

Fig. 1. Schematic diagram of human urinary kallidinogenase (KN) hydrolyzing substrate S-2266.

wavelengths for pNA, S-2266, and KN were 380 nm, 315 nm, and 280 nm, respectively (Fig. 3). Given the significant differences in their absorption characteristics, it was impractical to achieve optimal sensitivity for all analytes using a single detection wavelength. To enhance the signal-to-noise ratio and improve overall detection performance including recognition capacity, a multi-wavelength detection strategy was adopted. Consequently, detection wavelengths of 380 nm, 315 nm, and 280 nm were selected for pNA, S-2266, and KN, respectively.

3.2. Linearity and standard curves of pNA and S-2266

In the previously reported UV–Vis method [43], only the product pNA was used to quantify KN activity. However, since the product and substrate can be effectively separated and simultaneously detected in RP-HPLC, it is reasonable to propose that using pNA and S-2266 as dual indicators to determine KN enzyme activity would greatly enhance the reliability of quantification. Therefore, a dual-parameter quantification approach, based on the simultaneous measurement of product formation and substrate consumption, was adopted in this study. Standard curves of pNA and S-2266 were subsequently established.

Standard solutions of pNA and S-2266 at various concentrations were each injected in triplicate under the optimized chromatographic conditions, and the resulting chromatograms are shown in Fig. 4. The relationships between concentration and peak area for both analytes were plotted (Fig. S2), and the linear regression equations were determined using the least squares method.

The results showed that pNA exhibited excellent linearity over the concentration range of 0.05–100 μg•mL^{-1}, with a correlation coefficient (R^2) of 0.9999. Similarly, S-2266 demonstrated excellent linearity over the concentration range of 0.5–500 μg•mL^{-1}, with an R^2 of 0.9998. The limits of detection (LOD) for pNA and S-2266 were 0.01 μg•mL^{-1} and 0.25 μg•mL^{-1}, and the limits of quantification (LOQ) were 0.05 μg•mL^{-1} and 0.5 μg•mL^{-1}, with relative standard deviations (RSDs) of 0.97 % and 1.65 %, respectively (Table S2).

3.3. Evaluation of reaction time

The in vitro enzyme-catalyzed hydrolysis reaction of KN was evaluated through enzyme kinetics. The concentration of S-2266 was maintained at 1.5 mmol•L^{-1}, while various concentrations (2.5, 5.0, 7.5, 10.0, 12.5, 15.0, 17.5, and 20.0 μg•mL^{-1}) of KN solutions were used to perform the enzyme-catalyzed hydrolysis reaction over different time intervals (5, 10, 15, 20, 25, and 30 min), according to the protocol described in Section 2.6. All blank and reaction solutions were analyzed under optimized chromatographic conditions. A reaction progress curve was constructed based on the signal response of the product (pNA) (Fig. 5A), and a substrate consumption curve was established using the signal response of the substrate (S-2266) (Fig. 5B).

It was evident that a linear relationship existed between reaction time (2.5–30 min) and the peak areas of pNA and S-2266 at most KN concentrations, except at 2.5, 17.5, and 20 μg•mL^{-1}. The corresponding linear regression equations are detailed in Table 1. Linear regression analysis indicated that, within the selected time range, the peak areas of both the product (pNA) and the substrate (S-2266) exhibited excellent linearity with reaction time, reflecting a constant reaction rate. This phenomenon is consistent with zero-order reaction kinetics, suggesting that the reaction conditions are suitable for enzyme activity determination. Considering its applicability across various KN concentrations, a reaction time of 15 min was selected for subsequent enzyme activity determination, as it ensured reaction stability, sufficient product formation, and adequate substrate consumption, thereby enabling accurate determination of KN activity.

3.4. Evaluation of enzyme concentration

It is known that if the enzyme concentration is too high, it may lead to a falsely low measurement of enzyme activity due to the rapid consumption of substrates. On the contrary, if the enzyme concentration is too low, it may not effectively catalyze the reaction, resulting in inaccurate measurement results. Therefore, selecting an appropriate enzyme concentration is crucial. To ascertain the appropriate concentration range of KN for the enzyme activity determination, a series of KN concentrations ranging from 0.5 μg•mL^{-1} to 100 μg•mL^{-1} were employed in the enzyme-catalyzed hydrolysis reaction for 15 min, following the protocol described in Section 2.6.

The enzyme concentration optimization curves were established by plotting KN concentrations against the corresponding peak areas of the product (pNA) (Fig. 6). It was found that when the enzyme concentration was too low (0.5–2.5 μg•mL^{-1}), the relationship between peak area and enzyme concentration was nonlinear, indicating that the enzymatic reaction was insufficient. Therefore, enzyme activity could not be accurately determined at such low concentrations. Conversely, when the enzyme concentration was too high (20.0–100 μg•mL^{-1}), the reaction proceeded too rapidly, and the product peak areas quickly reached a plateau. The substrate concentration was no longer significantly greater than the Michaelis constant (K_m), causing the reaction kinetics to deviate from zero-order kinetics, making these conditions unsuitable for determining enzyme activity.

In contrast, within the concentration range of 2.5–20 μg•mL^{-1}, a strong linear relationship was observed between enzyme concentration and the peak area of pNA ($y = 23.6448\times$-17.9247, $R^2 = 0.9935$), suggesting this range is suitable for the determination of KN enzyme activity. Therefore, a concentration interval of 2.5–20 μg•mL^{-1} was selected for the analysis of KN samples.

3.5. Precision and trueness

The Michaelis-Menten Eq. [44] describes the kinetics of enzyme

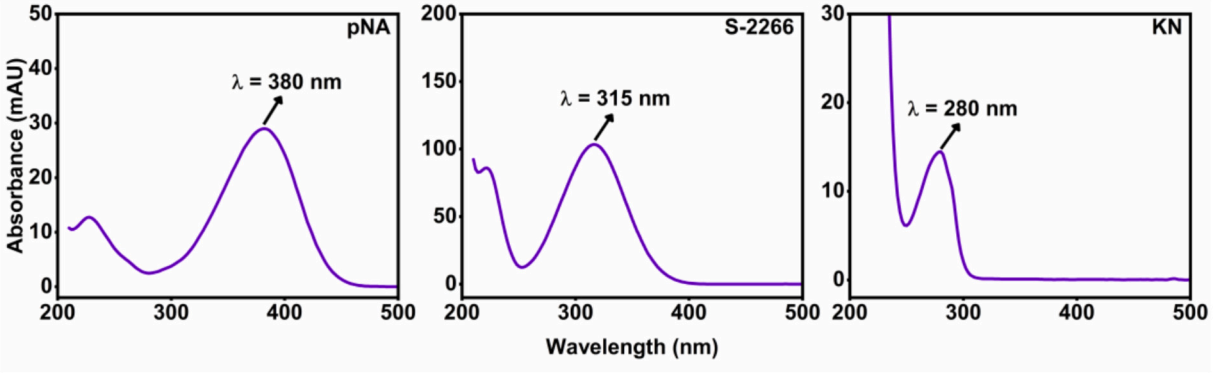

Fig. 3. UV–Vis absorption spectra of pNA, S-2266, and KN.

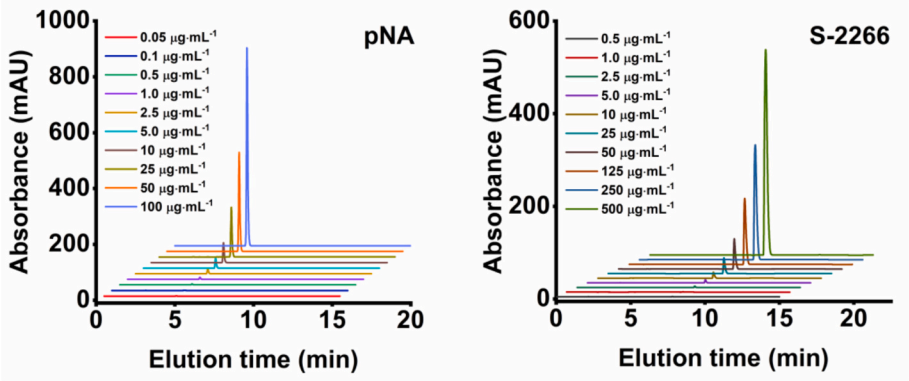

Fig. 4. HPLC chromatograms of pNA and S-2266 at various concentrations. Chromatograms were obtained on a TSKgel C4 column (4.6 × 150 mm i.d., 3 μm) at 30 °C, under a gradient condition: 0–5 min, linear gradient from A:B (20:80, v/v) to A:B (30:70, v/v); 5–10 min, linear gradient from A:B (30:70, v/v) to A:B (50:50, v/v); 10–15 min, isocratic elution at A:B (50:50, v/v). Mobile phase A was acetonitrile and mobile phase B was 0.1 % TFA aqueous solution at a flow rate of 1.0 mL min^{-1}. 10 μL aliquot of each standard solution was injected. Detection wavelengths were set at 380, and 315 nm for pNA, and S-2266, respectively.

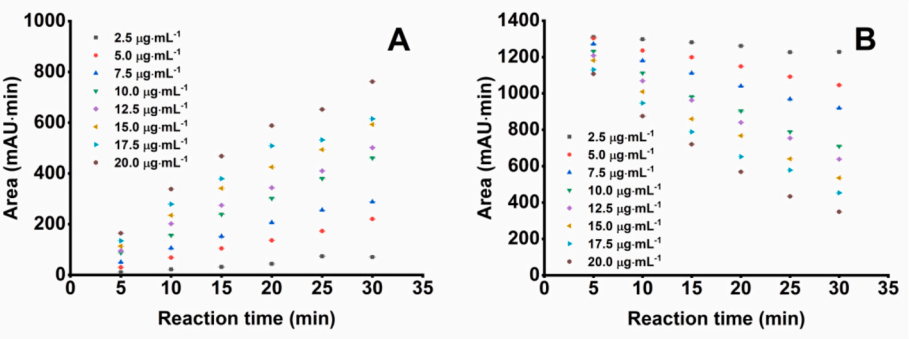

Fig. 5. Reaction progress curve (A) and substrate consumption curve (B) at various KN concentrations.

Table 1
Linear equations of reaction progress curve and substrate consumption curve at various enzyme concentrations.

Enzyme concentration ($\mu g \bullet mL^{-1}$)	Linear equation of reaction progress curve	R^2	Linear equation of substrate consumption curve	R^2	Linear range (min)
2.5	y = 2.1987 x - 0.0777	0.9994	y = −3.2119 x + 1327.2070	0.9922	2.5–20
5.0	y = 7.4649 x - 7.5872	0.9973	y = −9.5186 x + 1333.2066	0.9950	2.5–30
7.5	y = 9.6788 x - 4.3362	0.9974	y = −14.4311 x + 1329.2302	0.9983	2.5–30
10.0	y = 14.8194 x + 13.6464	0.9997	y = −21.9108 x + 1337.1382	0.9984	2.5–30
12.5	y = 15.3410 x + 39.0530	0.9933	y = −22.2657 x + 1304.7511	0.9970	2.5–30
15.0	y = 18.1635 x + 47.8447	0.9971	y = −24.3471 x + 1258.5026	0.9945	2.5–30
17.5	y = 24.6598 x + 14.8197	0.9975	y = −31.6607 x + 1276.3402	0.9952	2.5–20
20.0	y = 24.7667 x + 79.9637	0.9752	y = −35.3171 x + 1277.5394	0.9960	2.5–25

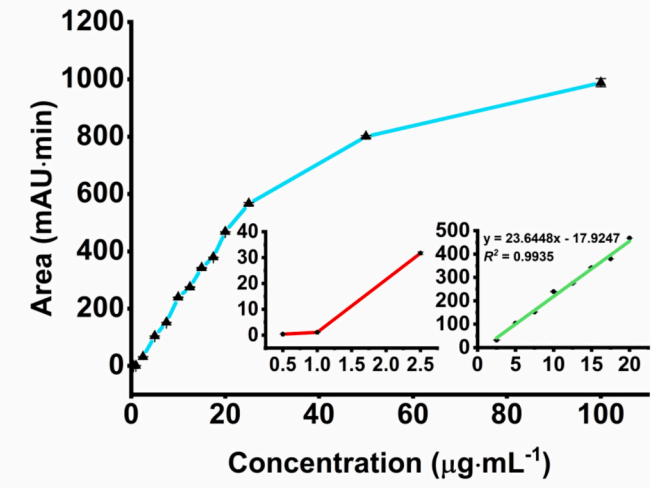

Fig. 6. Enzyme concentration optimization curves.

reactions (Eq. 1). The Michaelis constant (K_m, mol L^{-1}) is the substrate concentration at which the enzymatic reaction reaches half of its maximum rate (V_{max}, mol·L^{-1}·min^{-1}). When the substrate concentration (S, mol·L^{-1}) is much greater than the K_m, the reaction reaches its maximum reaction rate, and the initial rate (V_0, mol·L^{-1}·min^{-1}) approximates V_{max}. Under this condition, enzyme activity (U, mol·min^{-1}) can be determined based on the initial reaction rate (Eq. 2).

$$V_0 = \frac{V_{max} \times [S]}{K_m + [S]} \quad (1)$$

$$U = V_0 \times V_R = V_{max} \times V_R = \frac{\Delta C}{t} \times V_R \quad (2)$$

where,

V_R: Total reaction volume (L);

ΔC: Concentration change of the substrate during the reaction ($mol \cdot L^{-1}$);

t: Reaction time (min).

The enzyme activity of KN, as determined by pNA and S-2266, was calculated using their respective quantification equations (Eqs. 3 and 4). These equations were derived from Eq. 2 and the standard curves of pNA and S-2266. The final results are expressed as enzyme activity per unit mass.

$$U_{KN1} = \frac{A_{pNA} \times V_1}{K_{pNA} \times M_{pNA} \times t \times V_2} \quad (3)$$

$$U_{KN2} = \frac{(A_0 - A_{S-2266}) \times V_1}{K_{S-2266} \times M_{S-2266} \times t \times V_2} \quad (4)$$

where,

U_{KN1}: Enzyme activity of KN ($mol \cdot min^{-1} \cdot mg^{-1}$) determined by pNA;

U_{KN2}: Enzyme activity of KN ($mol \cdot min^{-1} \cdot mg^{-1}$) determined by S-2266;

V_1: Total reaction volume (μL);

V_2: Volume of enzyme solution (μL);

t: Reaction time (min);

A_0: Initial peak area of the substrate (S-2266) (mAU·min);

A_{pNA}: Peak area of the product (pNA) (mAU·min);

A_{S-2266}: Peak area of the substrate (S-2266) (mAU·min);

K_{pNA}: Slope of the pNA standard curve;

K_{S-2266}: Slope of the S-2266 standard curve;

M_{pNA}: Relative molecular weight of pNA ($g \cdot mol^{-1}$);

M_{S-2266}: Relative molecular weight of S-2266 ($g \cdot mol^{-1}$).

Chromatograms of the blank and reaction solution are shown in Fig. S3. The results demonstrate that the product (pNA) and the substrate (S-2266) were successfully separated and quantified in the reaction solutions, while only the substrate (S-2266) was detected and quantified in the blank solution. However, KN itself was not detected due to its very low concentration (<1.3 μg•mL^{-1} in actual HPLC injection solution).

To evaluate the precision and trueness of the dual-parameter quantitative method for KN activity determination, both intra-day and inter-day reproducibility studies were conducted. Each assessment included four independent experiments.

The intra-day RSDs for determining KN activity using pNA and S-2266 as indicators were 0.54 % and 0.52 %, respectively. The inter-day RSDs were 1.51 % and 0.51 %, respectively (Table 2). These results suggest that the method possesses good precision, satisfying the criteria for analytical reproducibility. Notably, data in Table 2 also showed that the enzyme activity of KN in the real sample was 5.07 ± 0.03 and 5.11 ± 0.07 $mol \cdot min^{-1} \cdot mg^{-1}$ on the same day, and 5.24 ± 0.08 and 5.23 ± 0.03 $mol \cdot min^{-1} \cdot mg^{-1}$ on different days calculated based on pNA and S-2266, respectively, demonstrating a high level of consistency between the two quantification indicators.

Table 2
The intra-day and inter-day determination of enzyme activity of KN.

	U_{pNA}	Mean ± SD	RSD	U_{S-2266}	Mean ± SD	RSD
	$mol \cdot min^{-1} \cdot mg^{-1}$		%	$mol \cdot min^{-1} \cdot mg^{-1}$		%
intra-day (*n* = 4)	5.10, 5.04 5.06, 5.08	5.07 ± 0.03	0.54	5.17, 5.16 5.00, 5.12	5.11 ± 0.07	0.52
inter-day (n = 4)	5.19, 5.29 5.32, 5.16	5.24 ± 0.08	1.51	5.24, 5.21 5.21, 5.27	5.23 ± 0.03	0.52

U_{pNA}: KN activity determined by pNA; U_{S-2266}: KN activity determined by S-2266.

Subsequently, a paired-sample *t*-test was conducted to compare the enzyme activity measurements obtained using the two parameters—the product and the substrate—based on eight sets of data from KN samples (Table 2). The mean enzyme activity of KN determined using the product as the parameter was U = 5.16 with a standard deviation (SD) of 0.10. The mean enzyme activity of KN determined using the substrate as the parameter was U = 5.17 with a standard deviation (SD) of 0.08. The statistical analysis revealed no significant difference between the two quantification parameters (product pNA vs. substrate S-2266): $t\ (7) = -0.558$, $p = 0.5954$ ($p > 0.05$), with a small effect size ($d = -0.197$) and a 95 % confidence interval of [−0.092, 0.057].

Bland-Altman plot analysis showed that all data points fell within the limits of agreement, further validating the consistency between the quantification methods based on the product (pNA) and the substrate (S-2266) (Fig. 7).

These crossing validation results demonstrate that the dual-parameter quantification method is accurate, reliable, and produces highly consistent enzyme activity values.

3.6. Greenness assessment of the procedure

Green chemistry [45] is increasingly recognized as a key principle in analytical science for minimizing environmental impact. Multiple evaluation tools have been developed to quantitatively assess the greenness of analytical methods, including AGREE [46], AGREEprep [47], CACI [48], AGSA [49], and MoGAPI [50]. In this study, all these tools were employed to evaluate the greenness of the proposed method, with the results summarized in Fig. 8.

Notably, the method achieved identical scores of 0.7 by using AGREE and AGREEprep. The AGREE tool rigorously assessed the solvent consumption, waste generation, number of operational steps, and energy usage throughout the analytical procedure. The score of our method was primarily affected by waste generation and the use of hazardous reagents in the mobile phase. The AGREEprep mainly evaluated the sample preparation process. No polluting reagents were employed during the preparation process in this work, reflecting a relatively green

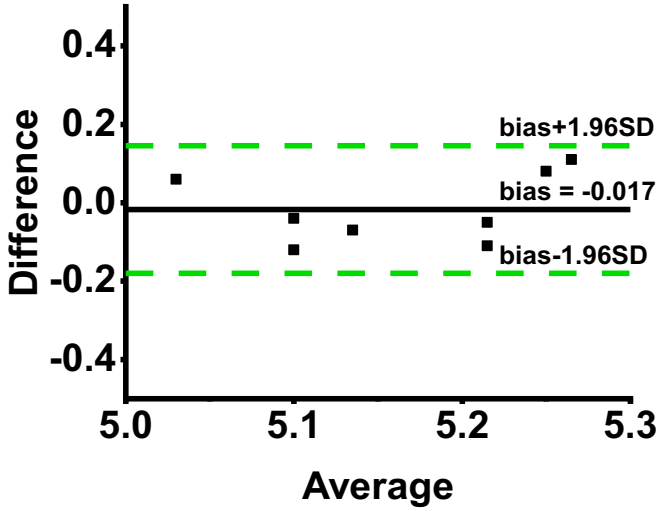

Fig. 7. Bland-Altman plot for the dual-parameter enzyme activity determination method.

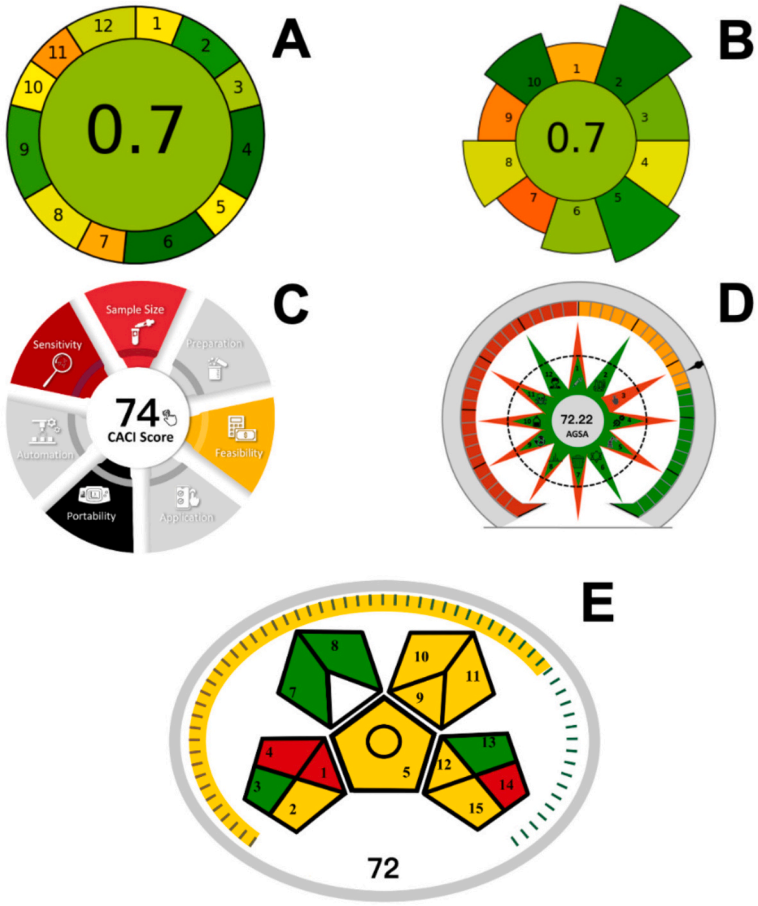

Fig. 8. Greenness assessment of the proposed method using different evaluation tools: (A) AGREE, (B) AGREEprep, (C) CACI, (D) AGSA, and (E) MoGAPI pictograms.

nature of the procedure. However, the total score was constrained by the fully manual execution of the sample preparation. As for the CACI, AGSA, and MoGAPI analyses, comprehensive scores of 74, 72.22, and 72 were obtained, respectively. These tools not only emphasize environmental impact but also comprehensively consider factors such as automation potential, operational simplicity, time efficiency, and analytical performance, thereby offering a balanced assessment of both greenness and practical applicability.

Overall, although the evaluation criteria of the five tools are different, the scores obtained were highly consistent. Compared with reported RP-HPLC methods [46,47,51,52], the proposed method demonstrated a relatively high greenness score. This method for determining KN enzyme activity exhibits distinct advantages in terms of sample pre-treatment, analytical throughput, sample consumption, and quantitation reliability.

4. Conclusions

A simple and accurate RP-HPLC method was established to assay the enzyme activity of human urinary kallidinogenase (KN). Under optimized chromatographic conditions, the approach demonstrated an excellent separation efficiency. Liquid chromatographic separation effectively minimized matrix interference, and the application of multiple detection wavelengths significantly improved the recognizing ability with high detection sensitivity. The dual-parameter quantification strategy, which simultaneously analyzes both the product and the substrate, was successfully applied to reliably determine KN activity. In addition, the simple sample pre-treatment, low sample usage, and efficient analysis positively contributed to the greenness of the method. In summary, the proposed RP-HPLC dual-parameter quantification method serves as an effective and dependable quality control tool for the production of KN and its final drug products. Moreover, this method exhibits potential for determining KN enzyme activity in complex matrices due to its remarkable sensitivity and strong analytical performance.

CRediT authorship contribution statement

Hong-yan Ge: Writing – original draft, Validation, Methodology, Investigation, Formal analysis, Data curation. **Ya-jun Zhang:** Validation, Investigation. **Jun-qin Qiao:** Writing – review & editing, Validation, Resources, Project administration, Funding acquisition, Formal analysis. **Li Fan:** Validation, Investigation. **He-liang Fu:** Supervision, Resources, Investigation. **Hong-zhen Lian:** Writing – review & editing, Supervision, Project administration, Funding acquisition, Conceptualization.

Declaration of competing interest

The authors declare that they have no known competing financial interests or personal relationships that could have appeared to influence the work reported in this paper.

Acknowledgments

This work was supported by the National Key Research and

Development Program of China (No. 2021YFF0600800), the National Natural Science Foundation of China (22304075, 22176085 and 21874065).

Appendix A. Supplementary data

Supplementary data to this article can be found online at https://doi.org/10.1016/j.jchromb.2025.124847.

Data availability

Data will be made available on request.

References

[1] M. Kesik-Brodacka, Progress in biopharmaceutical development, Biotechnol. Appl. Biochem. 65 (2018) 306–322, https://doi.org/10.1002/bab.1617.

[2] F. Roth-Walter, I.M. Adcock, C. Benito-Villalvilla, R. Bianchini, L. Bjermer, G. Caramori, L. Cari, K.F. Chung, Z. Diamant, I. Eguiluz-Gracia, et al., Comparing biologicals and small molecule drug therapies for chronic respiratory diseases: an EAACI taskforce on immunopharmacology position paper, Allergy 74 (2019) 432–448, https://doi.org/10.1111/all.13642.

[3] C. Yewale, D. Baradia, I. Vhora, A. Misra, Proteins: emerging carrier for delivery of cancer therapeutics, Expert Opin. Drug Deliv. 10 (2013) 1429–1448, https://doi.org/10.1517/17425247.2013.805200.

[4] T. El-Shanawany, W.A.C. Sewell, S.A. Misbah, S. Jolles, Current clinical uses of intravenous immunoglobulin, Clin. Med. (Lond.) 6 (2006) 356–359, https://doi.org/10.7861/clinmedicine.6-4-356.

[5] J.L. Tullis, Albumin: 2, Guidelines for clinical use, JAMA 237 (1997) 460–463, https://doi.org/10.1001/jama.237.5.460.

[6] C.M. Heckmann, F. Paradisi, Looking back: a short history of the discovery of enzymes and how they became powerful chemical tools, Chem. Cat. Chem. 12 (2020) 6082–6102, https://doi.org/10.1002/cctc.202001107.

[7] E.T. Kaiser, D.S. Lawrence, S.E. Rokita, The chemical modification of enzymatic specificity, Annu. Rev. Biochem. 54 (1985) 565–595, https://doi.org/10.1146/annurev.bi.54.070185.003025.

[8] C. Adamson, M. Kanai, Integrating abiotic chemical catalysis and enzymatic catalysis in living cells, Org. Biomol. Chem. 19 (2021) 37–45, https://doi.org/10.1039/D0OB01898H.

[9] M. de la Fuente, L. Lombardero, A. Gómez-González, C. Solari, I. Angulo-Barturen, A. Acera, E. Vecino, E. Astigarraga, G. Barreda-Gómez, Enzyme therapy: current challenges and future perspectives, Int. J. Mol. Sci. 22 (2021) 9181, https://doi.org/10.3390/ijms22179181.

[10] L. Gremmler, S. Kutschan, J. Dörfler, J. Büntzel, J. Büntzel, J. Hübner, Proteolytic enzyme therapy in complementary oncology: a systematic review, Anticancer Res 41 (2021) 3213–3232, https://doi.org/10.21873/anticanres.15108.

[11] J. Leipner, F. Iten, R. Saller, Therapy with proteolytic enzymes in rheumatic disorders, Biodrugs 15 (2001) 779–789, https://doi.org/10.2165/00063030-200115120-00001.

[12] S.A. Farhadi, E. Bracho-Sanchez, S.L. Freeman, B.G. Keselowsky, G.A. Hudalla, Enzymes as immunotherapeutics, Bioconjug. Chem. 29 (2018) 649–656, https://doi.org/10.1021/acs.bioconjchem.7b00719.

[13] J.N. Hennigan, M.D. Lynch, The past, present, and future of enzyme-based therapies, Drug Discov. Today 27 (2022) 117–133, https://doi.org/10.1016/j.drudis.2021.09.004.

[14] M.J. Poznansky, Enzyme protein conjugates-new possibilities for enzyme therapy, Pharmacol. Ther. 21 (1983) 53–76, https://doi.org/10.1016/0163-7258(83)90067-0.

[15] B. Torres-Herrero, I. Armenia, C. Ortiz, J.M. de la Fuente, L. Betancor, V. Grazu, Opportunities for nanomaterials in enzyme therapy, J. Control. Release 372 (2024) 619–647, https://doi.org/10.1016/j.jconrel.2024.06.035.

[16] M. Yari, M.B. Ghoshoon, B. Vakili, Y. Ghasemi, Therapeutic enzymes: applications and approaches to pharmacological improvement, Curr. Pharm. Biotechnol. 18 (2017) 531–540, https://doi.org/10.2174/1389201018666170808150742.

[17] H.S. Lu, F.K. Lin, L. Chao, J. Chao, Human urinary kallikrein - complete amino acid sequence and sites of glycosylation, Int. J. Pept. Protein Res. 33 (1989) 237–249, https://doi.org/10.1111/j.1399-3011.1989.tb01277.x.

[18] N. Tomiya, J. Awaya, M. Kurono, H. Hanzawa, I. Shimada, Y. Arata, T. Yoshida, N. Takahashi, Structural elucidation of a variety of GalNAc-containing N-linked oligosaccharides from human urinary kallidinogenase, J. Biol. Chem. 1 (1993) 113–126, https://doi.org/10.1016/S0021-9258(18)54122-3.

[19] Z. Wei, Y. Lyu, X.L. Yang, X. Chen, P. Zhong, D.H. Wu, Therapeutic values of human urinary kallidinogenase on cerebrovascular diseases, Front. Neurol. 9 (2018) 403, https://doi.org/10.3389/fneur.2018.00403.

[20] A. Meani, C. Fabris, D. Vianello, A. Piccoli, G. Delfavero, R. Farini, A kinetic assay for human urinary kallikrein determination, Enzyme 33 (1985) 89–93, https://doi.org/10.1159/000469412.

[21] C.A. Palmerini, A. Datti, I.E. Vanderelst, L. Minuti, A. Orlacchio, An approach for fluorometric determination of glycosyltransferase activities, Glycoconj. J. 13 (1996) 631–636, https://doi.org/10.1007/BF00731451.

[22] Q. Hu, Y. Bao, S.Y. Gan, Y.W. Zhang, D.X. Han, L. Niu, Electrochemically controlled grafting of polymers for ultrasensitive electrochemical assay of trypsin activity, Biosens. Bioelectron. 165 (2020) 112358, https://doi.org/10.1016/j.bios.2020.112358.

[23] T. Chase, E. Shaw, Comparison of the esterase activities of trypsin, plasmin, and thrombin on guanidinobenzoate esters. Titration of the enzymes, Biochemistry 8 (1969) 2212, https://doi.org/10.1021/bi00833a063.

[24] L.I. Willems, H.S. Overkleeft, S.I. van Kasteren, Current developments in activity-based protein profiling, Bioconjug. Chem. 25 (2014) 1181–1191, https://doi.org/10.1021/bc500208y.

[25] X.D. Bi, Z. Liu, Enzyme activity assay of glycoprotein enzymes based on a boronate affinity molecularly imprinted 96-well microplate, Anal. Chem. 86 (2014) 12382–12389, https://doi.org/10.1021/ac503778w.

[26] X. Tong, S.Y. Shi, C.Y. Tong, A. Iftikhar, R.Q. Long, Y.F. Zhu, Quantum/carbon dots-based fluorescent assays for enzyme activity, Trac-Trends Anal. Chem. 131 (2020) 116008, https://doi.org/10.1016/j.trac.2020.116008.

[27] S. Sinharay, G. Fernández-Cuervo, J.P. Acfalle, M.D. Pagel, Detection of sulfatase enzyme activity with a CatalyCEST MRI contrast agent, Chem.-Eur. J. 22 (2016) 6491–6495, https://doi.org/10.1002/chem.201600685.

[28] T. de Rond, J. Gao, A. Zargar, M. de Raad, J. Cunha, T.R. Northen, J.D. Keasling, A high-throughput mass spectrometric enzyme activity assay enabling the discovery of cytochrome P450 biocatalysts, Angew. Chem.-Int. Edit. 58 (2019) 10114–10119, https://doi.org/10.1002/anie.201901782.

[29] P. Gago-Ferrero, A.A. Bletsou, D.E. Damalas, R. Aalizadeh, N.A. Alygizakis, H. P. Singer, J. Hollender, N.S. Thomaidis, Wide-scope target screening of >2000 emerging contaminants in wastewater samples with UPLC-Q-ToF-HRMS/MS and smart evaluation of its performance through the validation of 195 selected representative analytes, J. Hazard. Mater. 387 (2020) 121712, https://doi.org/10.1016/j.jhazmat.2019.121712.

[30] C. Ctortecka, N.M. Clark, B.W. Boyle, A. Seth, D.R. Mani, N.D. Udeshi, S.A. Carr, Automated single-cell proteomics providing sufficient proteome depth to study complex biology beyond cell type classifications, Nat. Commun. 15 (2024) 5707, https://doi.org/10.1038/s41467-024-49651-w.

[31] J.Z. Nordin, Y. Lee, P. Vader, I. Mäger, H.J. Johansson, W. Heusermann, O.P. B. Wiklander, M. Hällbrink, Y. Seow, J.J. Bultema, et al., Ultrafiltration with size-exclusion liquid chromatography for high yield isolation of extracellular vesicles preserving intact biophysical and functional properties, Nanomed.-Nanotechnol, Biol. Med. 11 (2015) 879–883, https://doi.org/10.1016/j.nano.2015.01.003.

[32] C. Cervia-Hasler, S.C. Brüningk, T. Hoch, B.W. Fan, G. Muzio, R.C. Thompson, L. Ceglarek, R. Meledin, P. Westermann, M. Emmenegger, et al., Persistent complement dysregulation with signs of thromboinflammation in active Long COVID, Science 383 (2024) eadg7942, https://doi.org/10.1126/science.adg7942.

[33] C.V.D. Padilha, G.A. Miskinis, M.E.A.O. de Souza, G.E. Pereira, D. de Oliveira, M. T. Bordignon-Luiz, M.D. Lima, Rapid determination of flavonoids and phenolic acids in grape juices and wines by RP-HPLC/DAD: method validation and characterization of commercial products of the new Brazilian varieties of grape, Food Chem. 228 (2017) 106–115, https://doi.org/10.1016/j.foodchem.2017.01.137.

[34] A. Tsiasioti, P.D. Tzanavaras, High performance liquid chromatography coupled with post - column derivatization methods in food analysis: chemistries and applications in the last two decades, Food Chem. 443 (2024) 138577, https://doi.org/10.1016/j.foodchem.2024.138577.

[35] C. Yuan, W.Y. Jia, Z.Y. Yu, Y.A. Li, M. Zi, L.M. Yuan, Y. Cui, Are highly stable covalent organic frameworks the key to universal chiral stationary phases for liquid and gas chromatographic separations, J. Am. Chem. Soc. 144 (2022) 891–900, https://doi.org/10.1021/jacs.1c11051.

[36] B.W.J. Pirok, D.R. Stoll, P.J. Schoenmakers, Recent developments in two-dimensional liquid chromatography: fundamental improvements for practical applications, Anal. Chem. 91 (2019) 240–263, https://doi.org/10.1021/acs.analchem.8b04841.

[37] M. Locatelli, A. Kabir, M. Perrucci, H.I. Ulusoy, S. Ulusoy, N. Manousi, V. Samanidou, I. Ali, S.I. Kaya, F.R. Mansour, et al., Recent trends in sampling and sorbent-based sample preparation procedures for bioanalytical applications, Microchem. J. 207 (2024) 111903, https://doi.org/10.1016/j.microc.2024.111903.

[38] M. Perrucci, E.M. Ricci, M. Locatelli, I. Ali, F.R. Mansour, A. Kabir, H.I. Ulusoy, Recent trends in microsampling and reduced-volume sample preparation procedures, Adv. Sample Prep. 14 (2025) 100182, https://doi.org/10.1016/j.sampre.2025.100182.

[39] H. Jiang, K.W. Yang, X.X. Zhao, W.Q. Zhang, Y. Liu, J.W. Jiang, Y. Cui, Highly stable Zr(IV)-based metal-organic frameworks for chiral separation in reversed-phase liquid chromatography, J. Am. Chem. Soc. 143 (2021) 390–398, https://doi.org/10.1021/jacs.0c11276.

[40] T. Ahmed, X.H. Sun, C.C. Udenigwe, Role of structural properties of bioactive peptides in their stability during simulated gastrointestinal digestion: a systematic review, Trends Food Sci. Technol. 120 (2022) 265–273, https://doi.org/10.1016/j.tifs.2022.01.008.

[41] L.P. de Souza, S. Alseekh, F. Scossa, A.R. Fernie, Ultra-high-performance liquid chromatography high-resolution mass spectrometry variants for metabolomics research, Nat. Methods 18 (2021) 733–746, https://doi.org/10.1038/s41592-021-01116-4.

[42] T.N. Guo, J.A. Steen, M. Mann, Mass-spectrometry-based proteomics: from single cells to clinical applications, Nature 638 (2025) 901–911, https://doi.org/10.1038/s41586-025-08584-0.

[43] B. Jovov, N.K. Wills, P.J. Donaldson, Vectorial secretion of a kallikrein-like enzyme by cultured renal-cells. 1. General-properties, Am. J. Physiol. 259 (1990) 869–882, https://doi.org/10.1152/ajpcell.1990.259.6.C869.

[44] K.A. Johnson, R.S. Goody, The original Michaelis constant: Translation of the, Michaelis-Menten paper, Biochemistry 50 (2011) (1913) 8264–8269, https://doi.org/10.1021/bi201284u.
[45] M. Locatelli, A. Kabir, M. Perrucci, S. Ulusoy, H.I. Ulusoy, I. Ali, Green tools: current status and future, Adv. Sample Prep. 6 (2023) 100068, https://doi.org/10.1016/j.sampre.2023.100068.
[46] F. Pena-Pereira, W. Wojnowski, M. Tobiszewski, AGREE-analytical GREEnness metric approach and software, Anal. Chem. 92 (2020) 10076–10082, https://doi.org/10.1021/acs.analchem.0c01887.
[47] W. Wojnowski, M. Tobiszewski, F. Pena-Pereira, E. Psillakis, AGREEprep - Analytical greenness metric for sample preparation, TrAC-Trends Anal. Chem. 149 (2022) 116553, https://doi.org/10.1016/j.trac.2022.116553.
[48] F.R. Mansour, A. Bedair, M. Locatelli, Click analytical chemistry index as a novel concept and framework, supported with open source software to assess analytical methods, Adv. Sample Prep. 14 (2025) 100164, https://doi.org/10.1016/j.sampre.2025.100164.
[49] F.R. Mansour, A. Bedair, F. Belal, G. Magdy, M. Locatelli, Analytical green star area (AGSA) as a new tool to assess greenness of analytical methods, Sustain. Chem. Pharm. 46 (2025) 102051, https://doi.org/10.1016/j.scp.2025.102051.
[50] F.R. Mansour, J. Plotka-Wasylka, M. Locatelli, Modified GAPI (MoGAPI) tool and software for the assessment of method greenness: case studies and applications, Analytica 5 (2024) 451–457, https://doi.org/10.3390/analytica5030030.
[51] M.W. Nassar, A. Serag, M.A. Hasan, M. Kamel, Development and validation of a RP-HPLC method for simultaneous determination of five COVID-19 antiviral drugs in pharmaceutical formulations, Sci. Rep. 15 (2025) 25470, https://doi.org/10.1038/s41598-025-09904-0.
[52] S.M. Mahgoub, F.M. Alminderej, A.Y. Binsaleh, B.R. Alsehli, S.M. Saleh, M. A. Mohamed, Green and white analytical approach for parallel quantification of gabapentin and methylcobalamin in medicinal products using inventive RP-HPLC technique, Sci. Rep. 15 (2025) 20263, https://doi.org/10.1038/s41598-025-07056-9.